



Patient-Specific Quality Assurance in a Multileaf Collimator-Based CyberKnife System Using the Planar Ion Chamber Array

Jeongmin Yoon*, Eungman Lee[†], Kwangwoo Park[†], Jin Sung Kim[†], Yong Bae Kim[†], Ho Lee[†]

*Department of Radiation Oncology, Seoul National University Hospital, [†]Department of Radiation Oncology, Yonsei University College of Medicine, Seoul, Korea

Received 24 May 2018

Revised 23 June 2018

Accepted 23 June 2018

Corresponding author

Ho Lee

(holee@yuhs.ac)

Tel: 82-2-2228-4363

Fax: 82-2-2227-7823

This paper describes the clinical use of the dose verification of multileaf collimator (MLC)-based CyberKnife plans by combining the Octavius 1000SRS detector and water-equivalent RW3 slab phantom. The slab phantom consists of 14 plates, each with a thickness of 10 mm. One plate was modified to support tracking by inserting 14 custom-made fiducials on surface holes positioned at the outer region of 10×10 cm². The fiducial-inserted plate was placed on the 1000SRS detector and three plates were additionally stacked up to build the reference depth. Below the detector, 10 plates were placed to avoid longer delivery times caused by proximity detection program alerts. The cross-calibration factor prior to phantom delivery was obtained by performing with 200 monitor units (MU) on the field size of 95×92.5 mm². After irradiation, the measured dose distribution of the coronal plane was compared with the dose distribution calculated by the MultiPlan treatment planning system. The results were assessed by comparing the absolute dose at the center point of 1000SRS and the 3-D Gamma (γ) index using 220 patient-specific quality assurance (QA). The discrepancy between measured and calculated doses at the center point of 1000SRS detector ranged from -3.9% to 8.2%. In the dosimetric comparison using 3-D γ -function (3%/3 mm criteria), the mean passing rates with γ -parameter ≤ 1 were 97.4% \pm 2.4%. The combination of the 1000SRS detector and RW3 slab phantom can be utilized for dosimetry validation of patient-specific QA in the CyberKnife MLC system, which made it possible to measure absolute dose distributions regardless of tracking mode.

Keywords: CyberKnife, MLC, Patient-specific quality assurance, Octavius 1000SRS

Introduction

The CyberKnife (Accuray Inc., Sunnyvale, CA, USA) system is designed for robotic radiosurgery and stereotactic body radiotherapy. Its intrafraction motion tracking abilities enable delivery of high doses of radiation in only a few fractions.¹⁾ Non-coplanar beams with sub-millimeter accuracy provide a highly conformal dose distribution. A newly released M6 model, 5th generation CyberKnife sys-

tem, makes it possible to use multileaf collimator (MLC).²⁾ In addition to conventional benefits of CyberKnife, the use of MLC can be expected to create fields that match the tumor shape closely and spare critical organs, providing better dose distributions with an advantage in reducing beam delivery time.^{3,4)} The good candidates for the MLC system can be thus considered as the treatment of large targets or targets near critical organs. However, the new MLC system has all the potential issues like other MLC deliveries that

small changes in field size, dose rate, and MLC speed for each segment can significantly affect the dose accuracy. A few fractions indicate fewer chances to catch errors during treatment. In addition, Task Group (TG) 135 recommends that pretreatment delivery quality assurance (DQA) should be performed for every patient on a newly installed machine until the treatment team gets a good assessment.⁵⁾ At this point, it is essential to conduct at the same level of DQA that one would perform for linear accelerator IMRT or Tomotherapy patients,⁶⁾ until we have valuable data to judge the level of risk.

In this study, we focused on the clinical use of a 2D-array ion chamber with fiducial-inserted solid water phantom applicable to MLC-based CyberKnife system. The Octavius 1000SRS detector (PTW, Freiburg, Germany) as 2D-array ion chamber was used in linear accelerator for dosimetric measurement.⁷⁾ In the treatment planning system for CyberKnife, the presence of fiducial is important to generate patient-specific QA plan because the coincidence of tracking method is only compatible to make QA plans except the fiducial method. We designed the customized 14 fiducial-inserted slab phantom to support fiducial tracking with the Octavius 1000SRS detector. To our knowledge, this is the first study using high sensitive 2D ion chamber array detector that has evaluated the clinical application of measurement-based patient-specific QA in the new CyberKnife MLC system.

Materials and Methods

1. Patient-specific QA phantom

1) Octavius 1000SRS detector

The characteristics of Octavius 1000SRS were examined by Markovic et al.⁷⁾ The detector has a high resolution region, 2.5 mm, in the size of 5.5×5.5 cm² and a lower resolution region, 5 mm, in outer field size. And the maximum field size of detector is 11×11 cm². The 2D array consists of 977 liquid-filled ionization chambers. The dimension of each detector is 2.3 mm×2.3 mm×0.5 mm. The reference point of measurement is positioned at 9.0 mm below the surface of the array. The Octavius detector is controlled by the VeriSoft software (PTW, Freiburg, Germany), which is used during measurement acquisition and analysis of the measurements. The software provides the evaluation tools such as profile comparison, planar isodose overlay, and gamma index calculation.

2) Design of fiducial-inserted RW3 Solid Water

Because fiducial tracking is compatible regardless of tracking modes used in the patient plans, we designed the customized fiducial-inserted RW3 Solid Water (PTW Freiburg, Freiburg, Germany). The physical density of RW3 is 1.045 g/cm³, the effective material parameter $(Z/Ar)_{\text{eff}}$ is 0.536 and the electron density is higher than that of water by a factor of 1.012. 14 white golds as fiducials were inserted on the surface of RW3 as shown in Fig. 1. Among 14 fiducials, more than one fiducial can be required for tracking in the target zone during beam delivery. Previously-

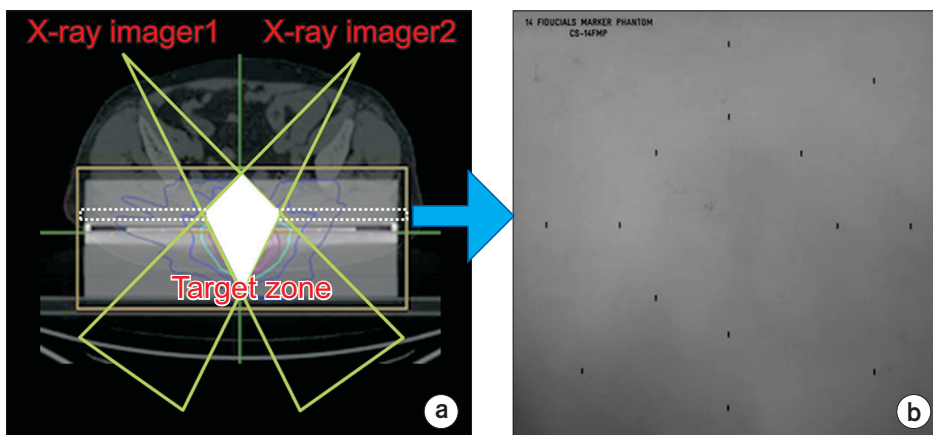


Fig. 1. The position of fiducial-inserted RW3 slab in patient-specific QA phantom: (a) Target zone overlapped by two x-ray imagers and (b) RW3 plate including 14 custom-made fiducials.

used fiducial plate has four fiducials in a plate. It could not be used any more left or right shifted cases because the target zone is fixed at machine center.

3) Patient-specific QA phantom setup

14 RW3 slabs were set up to measure the dose distribution from coronal plan. The thickness of each plate is 10 mm. Only one plate was modified to support tracking by inserting 14 customized fiducials on surface hole where the fiducials are orthogonally positioned on outer region of array. As shown in Fig. 2, the modified plate was placed on the Octavius 1000SRS detector. 10 slabs below 1000SRS detector were placed to avoid longer delivery times caused by proximity detection program alerts. Three slabs were stacked up on the modified plate to build the reference depth.



Fig. 2. Patient-specific QA phantom including fiducial-inserted solid water phantom and Octavius 1000SRS detector.

2. Generation of QA template plan

MultiPlan 5.1.2 treatment planning system (Accuray Inc., Sunnyvale, CA, USA), used with Cyberknife MLC system, provides the finite size pencil beam (FSPB) algorithm for the final dose calculation. Five tracking methods^{8,9)} were supported by the MultiPlan: Fiducial, Synchrony, Xsight Lung, Xsight Spine and 6D Skull. Most methods use the same tracking method for both patient plan and QA template plan as shown in Table 1. However, when QA template plan is created using fiducial tracking, it is compatible to all of tracking method for patient plans. In the target zone, the fiducial could be the identified by fiducial finder in MultiPlan system (Fig. 3a).

3. DQA plan and delivery

DQA plan procedure began with selecting the volume of interest (VOI) (Fig. 3b) at the patient plan and then exact alignment of the VOI at the QA template plan was performed. Next, the dose calculation for DQA plan was performed by using the same patient plan data such as beam data, system data, path set, anatomy center, and reference point. After then, rescale of monitor unit (MU) was required for delivery time reduction. Finally the calculated 3D dose distributions were exported from MultiPlan (Fig. 4). The cross-calibration factor prior to phantom delivery was obtained by performing with 200 MU on the field size of $95 \times 92.5 \text{ mm}^2$.

Table 1. Tracking mode compatibility between patient plan and QA template plan.

Tracking method	QA template plan Fiducial	QA template plan Synchrony	QA template plan Xsight Lung	QA template plan Xsight Spine	QA template plan 6D Skull
Patient Plan Fiducial	Compatible				
Patient Plan Synchrony	Compatible (with warning)	Compatible			
Patient Plan Xsight Lung	Compatible (with warning)		Compatible		
Patient Plan Xsight Spine	Compatible (with warning)			Compatible	
Patient Plan 6D Skull	Compatible (with warning)				Compatible

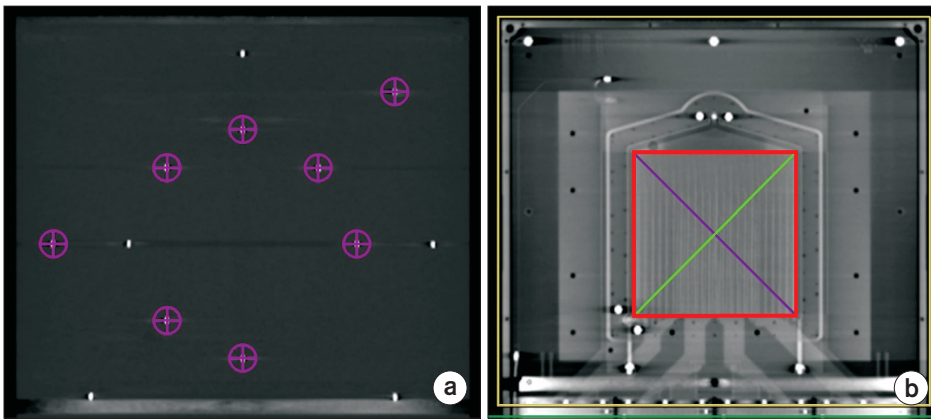


Fig. 3. QA template plan: (a) Fiducial identifications in fiducial-inserted RW3 plate and (b) a volume of interest representing ion chamber array.

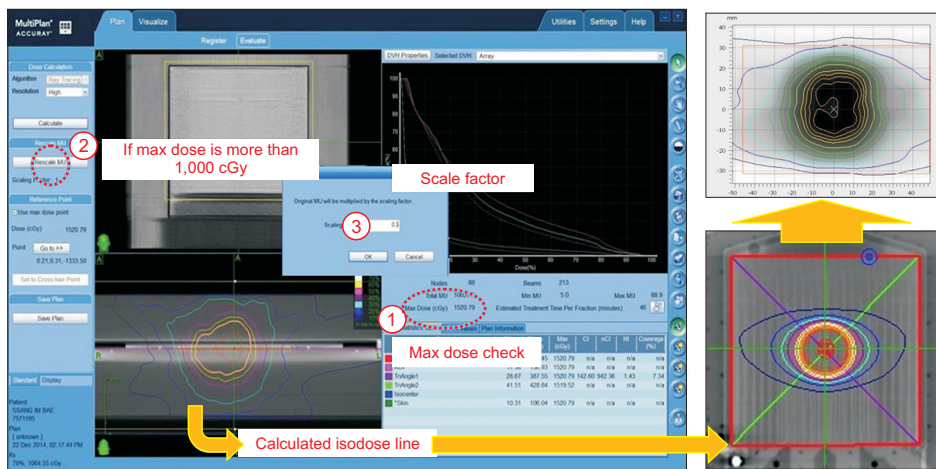


Fig. 4. Procedures to export the calculated 3D dose distribution in MultiPlan TPS.

Table 2. The number of cases used for patient-specific QA.

Tracking method	Number of case
Fiducial	10
Synchrony	4
Xsight Lung	2
Xsight Spine	196
6D Skull	8

4. Analysis of DQA plan and delivery

We analyzed 220 intracranial and extracranial cases using MLC. The number of cases using different tracking methods is shown in Table 2. Among five tracking methods, the Xsight Spine tracking method was mostly used in this study (Table 2). The measured dose distribution of coronal plane (2-D array after DQA plan delivery) was compared with the 3D dose distribution calculated by MultiPlan for cross-validation (Fig. 5). We evaluated point dose differ-

ence (%) at the center of Octavius 1000SRS and 3D gamma (γ) index agreement. The γ function criteria is based on the distance-to-agreement of 3 mm and the local dose difference of 3%.¹⁰⁾

Results

The overall point dose difference between measured and calculated doses ranged from -3.9% and 8.2 % in Fig. 6a. The mean point dose difference was $2.3\% \pm 2.3\%$. As shown in Fig. 6b, the mean passing rates with $\gamma \leq 1$ were $97.4\% \pm 2.4\%$ in coronal plane. The lowest and highest gamma agreements were 90% and 100%, respectively. Also, the difference of point dose and gamma passing ratio was analyzed according to the tracking method (Table 3). For representative partial breast irradiation (PBI) patients with surgical clips, fiducial tracking was used. In this tracking method, the difference of point dose and gamma passing

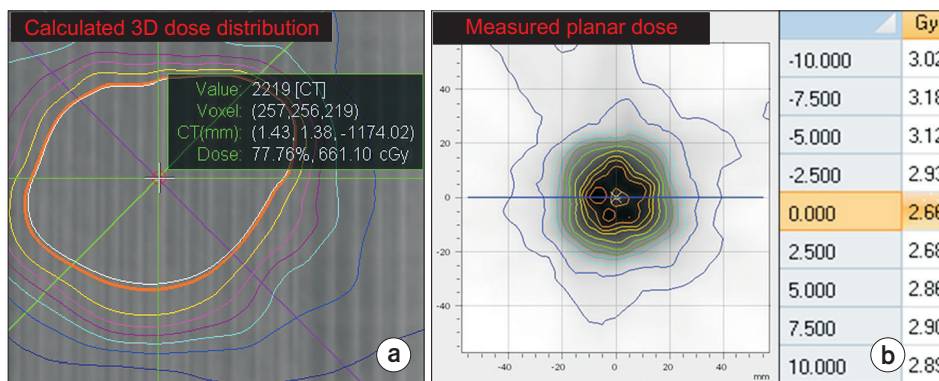


Fig. 5. Comparison between measured planar dose and calculated 3D dose distributions: (a) calculated point dose at the center of Octavius 1000SRS detector and (b) measured planar dose distribution in Verisoft.

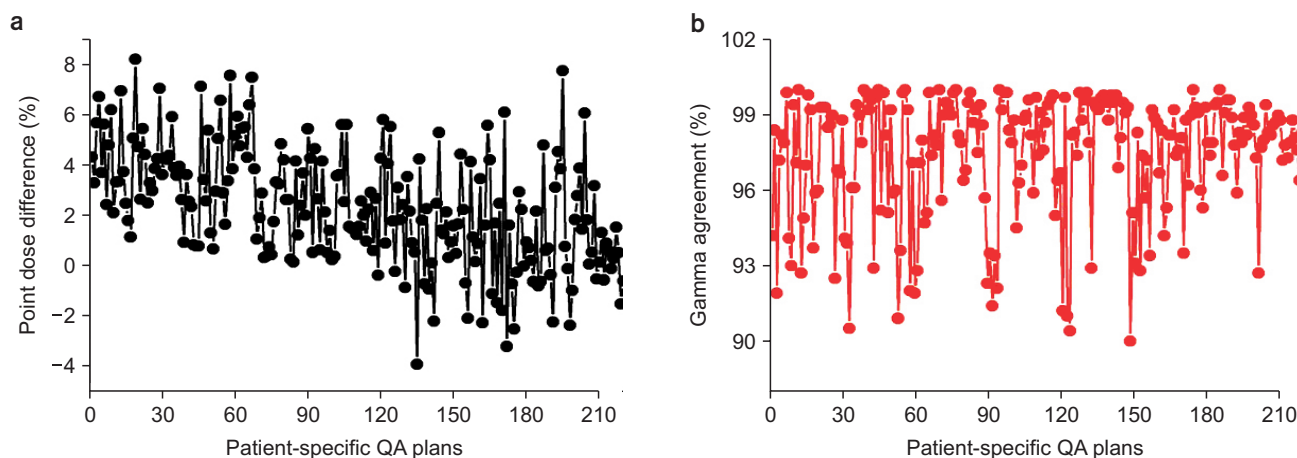


Fig. 6. Quantitative comparisons using 220 patient specific QA plans: (a) point dose difference and (b) gamma agreement.

Table 3. The Results for patient-specific QA.

Tracking method	Point dose difference (%)	Gamma passing ratio (%)
Fiducial	4.24±2.27	97.05±2.77
Synchrony	0.84±2.30	98.40±0.83
Xsight Lung	1.34±0.18	98.95±1.06
Xsight Spine	2.30±2.35	98.20±2.47
6D Skull	2.68±1.82	97.70±1.96

ratio was 4.24%±2.27% and 97.05%±2.77%, respectively. For PBI or liver patients with synchrony tracking, the difference of point dose and gamma passing ratio showed 0.84%±2.30% and 98.40%±0.83%. For lung treatment with high fractional dose (over 1500 cGy) with synchrony, Xsight Lung tracking was performed on the patient plan. The difference of point dose and gamma passing ratio showed 1.34%±0.18% and 98.95%±1.06%. For C-spine or T-spine treatment, Xsight Spine tracking was used dominantly, which showed 2.30%±2.35% and 98.20%±2.47% for the dif-

ference of point dose and gamma passing ratio. For brain treatment, 6D Skull tracking was selected. Using this tracking, the difference of point dose and gamma passing ratio showed 2.68%±1.82% and 97.70%±1.96%.

Discussion

The current work focused on the MLC-based CyberKnife system. We performed the dose calculations with FSPB algorithm, which is available in the MultiPlan for MLC-based CyberKnife system. Additionally, the results of this work can be extended to the cone-based CyberKnife treatment using ray tracing or Monte Carlo algorithms in MultiPlan system.

There are other dosimetry tools that have the potential for CyberKnife delivery measurements.¹¹⁻¹³ 2D film dosimetry offers superior spatial resolution for small field measurements, but the resulting dose distributions are sensi-

tive to the handling method. Various electronic measuring devices are thus considered because they are capable for time-resolved analysis despite the limited spatial resolution. Compared with the electronic dosimetry devices such as MatriXX and ArcCHECK¹²⁾, the Octavius 1000SRS detector has a great advantage in cases involving the measurement of the high resolution dose distributions especially in high dose gradient regions because the spacing between ion chambers is 2.5 mm in the central area (the field size of 5.5×5.5 cm²). In addition, the workload can be reduced since dose distributions are acquired, shown, and can be processed at once. The acquisition software, VeriSoft, can provide the graphical environment for the comparison and evaluation of the dose distributions. Also, the measured data can be saved in different formats for the analysis. For the limitation of detector size (2.3 mm×2.3 mm×0.5 mm) of Octavius 1000 SRS, we considered the selection of the tumor size of patients which is larger than 1 cm. When we had the case of smaller than 1 cm, we used Stereotactic Dose Verification Phantom (Standard Imaging, WI, USA) with Exradin A16 microchamber (Standard Imaging, WI, USA) and customized Gafchromic EBT3 film (Ashland ISP Advanced Materials, NJ, USA).

The CyberKnife system has a predefined safety zone around the patient based on the patient's size. When we perform the patient-specific QA for a patient with the brain tumor, special attention is required to avoid the collision between the patient-specific QA phantom including Octavius 1000SRS detector and the moving robot arm due to the narrow patient safety zone.

Conclusion

We have demonstrated that the Octavius 1000SRS detector with fiducial-inserted RW3 slab phantom can be considered as a new dosimetric tool for robotic radiotherapy delivery QA. This combination made it reliable to measure absolute dose distributions regardless of tracking mode. It simultaneously achieved an accurate dosimetry validation of the noncoplanar delivery pattern.

Acknowledgements

This research was supported by Radiation Technology R&D program through the National Research Foundation of Korea funded by the Ministry of Science, ICT & Future Planning (NRF-2017M2A2A6A01070330) and by Basic Science Research Program through the National Research Foundation of Korea funded by the Ministry of Education (NRF-2015R1D1A1A01056850).

Conflicts of Interest

The authors have nothing to disclose.

Availability of Data and Materials

All relevant data are within the paper and its Supporting Information files.

References

1. Blomgren H, Lax I, Naslund I, Svanstrom R. Stereotactic high dose fraction radiation therapy of extracranial tumors using an accelerator. Clinical experience of the first thirty-one patients. *Acta Oncol.* 1995;34(6):861-70.
2. Yoon J, Park K, Kim JS, Kim YB, Lee H. Acceptance Testing and Commissioning of Robotic Intensity-Modulated Radiation Therapy M6 System Equipped with InCise™ 2 Multileaf Collimator. *Prog Med Phys.* 2018;29(1):8-15.
3. Murai T, Hattori Y, Sugie C, Iwata H, Iwabuchi M, Shibamoto Y. Comparison of multileaf collimator and conventional circular collimator systems in Cyberknife stereotactic radiotherapy. *J Radiat Res.* 2017;58(5):693-700.
4. Mcguinness CM, Gottschalk AR, Lessard E, et al. Investigating the clinical advantages of a robotic linac equipped with a multileaf collimator in the treatment of brain and prostate cancer patients. *J Appl Clin Med Phys.* 2015;16(5):284-95.
5. Dieterich S, Cavedon C, Chuang CF, et al. Report of AAPM TG 135: quality assurance for robotic radiosurgery. *Med Phys.* 2011;38(6):2914-36.
6. Chong NS, Lee JJS, Kung WH, et al. Patient delivery quality assurance for linac-based IMRT and helical tomotherapy

- using solid state detectors. *Radiat Meas.* 2011;46(12):1993-95.
7. Markovic M, Stathakis S, Mavroidis P, Jurkovic IA, Papanikolaou N. Characterization of a two-dimensional liquid-filled ion chamber detector array used for verification of the treatments in radiotherapy. *Med Phys.* 2014;41(5).
 8. Seppenwoolde Y, Berbeco RI, Nishioka S, Shirato H, Heijmen B. Accuracy of tumor motion compensation algorithm from a robotic respiratory tracking system: A simulation study. *Med Phys.* 2007;34(7):2774-84.
 9. Pepin EW, Wu H, Zhang Y, Lord B. Correlation and prediction uncertainties in the cyberknife synchrony respiratory tracking system. *Med Phys.* 2011;38(7):4036-44.
 10. Ezzell GA, Burmeister JW, Dogan N, et al. IMRT commissioning: multiple institution planning and dosimetry comparisons, a report from AAPM Task Group 119. *Med Phys.* 2009;36(11):5359-73.
 11. Blanck O, Masi L, Damme MC, et al. Film-based delivery quality assurance for robotic radiosurgery: Commissioning and validation. *Phys Med.* 2015;31(5):476-83.
 12. Lin MH, Veltchev I, Koren S, Ma C, Li J. Robotic radiosurgery system patient-specific QA for extracranial treatments using the planar ion chamber array and the cylindrical diode array. *J Appl Clin Med Phys.* 2015;16(4):290-305.
 13. Kim J, Park K, Yoon J, et al. Feasibility Study of a Custom-made Film for End-to-End Quality Assurance Test of Robotic Intensity Modulated Radiation Therapy System. *Prog Med Phys.* 2016;27(4):189-95.